Heliyon 8 (2022) e12581

Contents lists available at ScienceDirect

Heliyon

journal homepage: www.cell.com/heliyon

Research article

N-alkylimidazole derivatives as potential inhibitors of quorum sensing in *Pseudomonas aeruginosa*

Caleb Nketia Mensah [a], Gilbert Boadu Ampomah [a], Jehoshaphat Oppong Mensah [a], Edward Ntim Gasu [a,b], Caleb Impraim Aboagye [a], Edmund Ekuadzi [b,c], Nathaniel Owusu Boadi [a], Lawrence Sheringham Borquaye [a,b,*]

[a] Department of Chemistry, Kwame Nkrumah University of Science and Technology, Kumasi, Ghana
[b] Central Laboratory, Kwame Nkrumah University of Science and Technology, Kumasi, Ghana
[c] Department of Pharmacognosy, Kwame Nkrumah University of Science and Technology, Kumasi, Ghana

ARTICLE INFO

Keywords:
Pyocyanin
LasR
Virulence factor
Biofilm inhibition
Imidazole derivatives

ABSTRACT

Antimicrobial resistance is a threat to global public health. Microbial resistance is mediated by biofilm formation and virulence behavior during infection. Quorum sensing (QS), a cell-to-cell communication is frequently used by microbes to evade host immune systems. Inhibiting QS channels is a potential route to halt microbial activities and eliminate them. Imidazole has been shown to be a potent warhead in various antimicrobial agents. This study aims to evaluate alkyl-imidazole derivatives as potential inhibitors of QS and to explore the interactions of the compounds with LasR, a key protein in the QS machinery of *Pseudomonas aeruginosa*. The study revealed that imidazole derivatives with longer alkyl chains possessed better antimicrobial activities. Octylimidazole and decylimidazole emerged as compounds with better anti-virulence and biofilm inhibition properties while hexylimidazole showed the best inhibitory activity against *Pseudomonas aeruginosa* PAO1. The binding affinity of the compounds with LasR followed a similar trend as that observed in the QS inhibitory assays, suggesting that interaction with LasR may be important for QS inhibition.

1. Introduction

Antimicrobial agents have greatly reduced illnesses and deaths from infectious diseases since their introduction. However, the outbreak of new infections, the re-emergence of old infections, the worrying trend of development of resistance to existing antimicrobial agents and the fall in new anti-infective drug discoveries, have all necessitated the quest for new antimicrobial therapeutics [1]. Antimicrobial resistance (AMR) remains a significant threat to global public health due to its contribution to increase in health cost and mortality rates. Globally, an estimated 10 million fatalities owing to AMR are projected by 2050, with Africa accounting for 4 million of them [2]. According to the United States' Centre for Disease Control and Prevention (CDC), more than 2 million antibiotic-resistant infections occur in the United States each year and more than 35,000 deaths are recorded as a result [3]. Due to a paucity of data, the present impact of AMR in Africa is uncertain, however there is evidence of considerable resistance to widely administered antibiotics [4].

The use of multiple antibiotics in combating antimicrobial resistance has led to the occurrence of multidrug resistance. Multidrug-resistant (MDR) microorganisms, such as methicillin-resistant *Staphylococcus aureus*, vancomycin-resistant enterococci [5, 6], extended-spectrum cephalosporin-resistant *Escherichia coli* and *Klebsiella* species [7, 8] and MDR *Pseudomonas aeruginosa* [9, 10] most frequently cause life-threatening diseases in humans. Recent reports of resistance means that treatment for severe infections for which some of these organisms are implicated may need to be initiated with different treatment options. Microorganisms have developed various strategies to overcome the action of some of these therapeutic agents. Some of such resistance strategies include the use of efflux pumps, functional group deactivation, and quorum sensing-mediated virulence factors expression such as biofilm formation [11].

Biofilm formation is a two-stage process that is mostly influenced by surface adhesins and quorum sensing (cell-to-cell communication) [12]. Biofilm associated microorganisms display decreased susceptibility to antimicrobial agents [13]. Most antimicrobial agents are unable to attack biofilms since they were designed to respond to planktonic organisms

* Corresponding author.
E-mail addresses: lsborquaye.sci@knust.edu.gh, slborquaye@gmail.com (L.S. Borquaye).

https://doi.org/10.1016/j.heliyon.2022.e12581
Received 26 July 2022; Received in revised form 20 October 2022; Accepted 15 December 2022

rather than biofilms (surface associated organisms). The protection provided by the biofilm could be the organism's own innate resistant mechanism or could be acquired through cell-to-cell communication where extra chromosomal elements are transferred to susceptible species in the biofilm [14]. Quorum sensing is, therefore, a mechanistic process that regulates biofilm formation. Quorum sensing (QS) is dependent on cell density and regulates several processes in bacteria such as biofilm formation, synthesis and secretion of virulence factors, motility, sporulation, antibiotic production, competence, bioluminescence, and exopolysaccharides synthesis. In many pathogenic microorganisms, the coordinated expression of virulence factors during infection of a host probably constitutes a significant survival advantage by enhancing the chances of establishing infection and escaping host immune response [15, 16]. *Pseudomonas aeruginosa* is a well characterized biofilm forming pathogen [17] which uses quorum sensing (QS) to control virulence factor production. In *P. aeruginosa*, four systems govern QS: las, rhl, Pseudomonas Quinolone Signal (PQS), and Integrated Quorum Sensing (IQS) (Thi, Wibowo and Rehm, 2020). The QS machinery in *P. aeruginosa* functions in a hierarchy, and at the top of this arrangement is the las system. The LasI synthase of *P. aeruginosa* produces autoinducer 3-oxo-C12-HSL (*N*-3-oxododecanoyl-L-homoserine lactone) which activates the LasR receptor. When activated, LasR binds to gene promoters and activates the transcription of genes crucial to the other QS systems – RhlR, PQS and IQS. In addition, genes that control the production of many toxic virulence factors and other functional molecules needed for biofilm development and maintenance are also expressed [18]. The virulence factors and functional molecules include the expression of pyoverdine, pyocyanin, rhamnolipid, polysaccharides and lectins. Inhibiting QS is a promising approach to counteract *P. aeruginosa* virulence factors and associated infections. Some of the approaches used in QS inhibition include harnessing natural products, structural modification of existing antibiotics and derivatization of various pharmacophores.

The imidazole core is an important pharmacophore found in many drugs [19]. Imidazole drugs have broad spectrum of action with pharmacological properties including antimycotic and antifungal, anthelmintic, antiprotozoal [20, 21]. Brahmbhat and coworkers synthesized derivatives of 3-(2-4-diphenyl-1H—imidazole-z-y)-1H-pyrazole and evaluated their antibacterial activity against *Staphylococcus aureus, Bacillus subtilis, Escherichia coli* and *P. aeruginosa*. They reported that the derivatives showed potent antibacterial activity which were comparable to standard drugs [22]. The antibacterial and antifungal properties of 3-biphenyl-3H-Imidazo[1,2-a]azepin-1-ium bromide derivatives have also been assessed, with some of the compounds showing broad activity against *S. aureus, C. neoformans* and *C. albicans* at minimum inhibitory concentrations ranging from 4 to 8 μg/mL [23]. Although the antibacterial activity of alkyl imidazoles have been reported [20], their ability to impact biofilm formation or QS-mediated processes have not been explored.

This study aims to investigate alkyl imidazole derivatives as modulators of biofilm formation and evaluates their ability to interfere with some QS-mediated processes. Alkyl derivatives of imidazole were synthesized from the condensation of appropriate alkyl bromides with imidazole. The crystal violet method was used to evaluate inhibition of biofilm formation. Interference with quorum sensing was evaluated by monitoring pyoverdine and pyocyanin expression in *P. aeruginosa*. Finally, a molecular docking analysis was performed utilizing the LasR protein to investigate the interactions of these compounds with the protein as a way of deciphering the potential pathways by which the compounds exert their effects.

2. Materials and methods

2.1. Materials

2.1.1. Chemicals

Imidazole, bromoethane, 1-bromopropane, 1-bomobutane, 1-bromopentane, 1-bromohexane, 1-bromooctane, 1-bromodecane, sodium chloride, sodium carbonate, acetone and all chemicals used were of analytical grade and were from Merck (Sigma-Aldrich), St. Louis, MO, USA, unless stated otherwise. Gentamicin was prepared in sterile MilliQ water.

2.1.2. Microorganisms

The antibacterial activity of the compounds was assessed against 4 Gram-negative and 3 Gram-positive bacteria. The Gram-negative bacteria used were *Pseudomonas* aeruginosa PAO1 (*P. aeruginosa*), *Escherichia coli* ATCC 25922 (*E. coli*), and *Escherichia coli* resistant strain (*E. coli-R*). Gram-positive bacteria included *Staphylococcus aureus* ATCC 25923 (*S. aureus*) and *Enterococcus faecalis* ATCC 29212 (*E. faecalis*) and Methicillin-resistant *Staphylococcus aureus* (MRSA). *Pseudomonas aeruginosa* PA01 strain was a kind donation from Prof. Scot Rice of the Nanyang Technological University, Singapore. All other strains were obtained from the Department of Pharmaceutical Microbiology, Kwame Nkrumah University of Science and Technology (KNUST).

2.2. Methods

2.2.1. General procedure for synthesis of alkyl imidazoles

To a solution of imidazole and potassium hydroxide (1:5 eq) in acetone was added the appropriate alkyl bromide at room temperature with continuous stirring for 30 min. The product was then isolated by extracting with ethyl acetate (3X) and the combined extract washed with brine. After drying over anhydrous sodium sulphate, the crude product was obtained by concentration *in vacuo* (Cole Parmer, USA). The crude product was purified using column chromatography (ethyl acetate: pet ether in a ratio of 7:3) before characterization.

2.3. Characterization of compounds

All alkyl imidazoles were characterized by ^{1}H NMR, ^{13}C NMR, IR, UV and GC-MS. ^{1}H NMR (500 MHz) and ^{13}C NMR (125 MHz) spectra were obtained in $CDCl_3$ at room temperature on a Bruker 500 MHz AVANCE III HD NMR spectrometer. The GC-MS spectra were recorded on a Perkin Elmer GC Clarus 580 Gas chromatograph interfaced with a Perkin Elmer (Clarus SQ 8 S) mass spectrometer. FT-IR Spectrophotometer (Bruker Alpha, Platinum ATR) was used for the IR analysis. UV-Vis spectrometer (Analytik Jena Specord 200 plus Double Beam) was used for the UV measurement. The spectra of all compounds are presented in Figures S1–S7.

2.3.1. 1-Ethyl-1H-imidazole (NEI)

pale-yellow oil. Yield: 51.08%. ^{1}H NMR (500 MHz, $CDCl_3$) δ 1.29 (t, J = 7.4 Hz, 3H), 3.82 (t, J = 7.4 Hz, 2H), 6.74 (s, 1H), 6.88 (s, 1H), 7.29 (s, 1H). ^{13}C NMR (125 MHz, $CDCl_3$) δ 15.3, 40.2, 118.69, 129.04, 136.92. IR (ν, cm^{-1}) ν = 3463.09, 2973–2932.14, 1698.69; λmax 212.0 nm. GC-EI-MS calculated molecular ion peak for $C_5H_8N_2$ 96.07 g/mol found *m/z* 96 (Figure S1).

2.3.2. 1-Propyl-1H-imidazole (NPrI).

pale-yellow oil. Yield: 63.32%. ^{1}H NMR (500 MHz, $CDCl_3$) δ 0.74 (t, J = 7.4 Hz, 3H), 1.62 (sx, J = 7.3 Hz, 2H), 3.71 (t, J = 7.1 Hz, 2H), 6.74 (s, 1H), 6.88 (s, 1H), 7.29 (s, 1H). ^{13}C NMR (125 MHz, $CDCl_3$) δ 10.9, 24.22, 48.48, 118.69, 129.04, 136.92. IR (ν, cm^{-1}) ν = 3385, 3108.97, 2958–2873, 1507.80; λmax 212.6 nm. GC-EI-MS calculated molecular ion peak for $C_8H_{14}N_2$ 109.21 g/mol, found *m/z* 109 (Figure S2).

2.3.3. 1-Butyl-1H-imidazole (NBI).

Yellowish oil. Yield: 53.83%. ^{1}H NMR (500 MHz, $CDCl_3$) δ 0.77 (t, J = 7.4 Hz, 3H), 1.14 (m, 2H), 1.58 (m, 2H), 3.76 (t, J = 7.1 Hz, 2H), 6.75 (s, 1H), 6.87 (s, 1H), 7.29 (s, 1H). ^{13}C NMR (125 MHz, $CDCl_3$) δ 13.34, 19.54, 32.90, 46.54, 118.69, 129.00, 136.88. IR (ν, cm^{-1}) ν = 3385.13, 2958–2932.68, 1507.08; λmax 212.6

nm. GC-EI-MS calculated molecular ion peak for $C_7H_{12}N_2$ 124.18 g/mol, found *m/z* 124 (Figure S3).

*2.3.4. 1-Pentyl-1H-imidazole (**NPnI**).* Yellowish oil. Yield: 55.64%. ^{1}H NMR (500 MHz, $CDCl_3$) δ 0.73 (t, J = 7.2 H, 3H), 1.23–1.05 (m, 4H), 1.60 (quint, J = 7.2 Hz, 2H), 3.75 (t, J = 7.1 Hz, 2H), 6.75 (s, 1H), 6.87 (s, 1H), 7.30 (s, 1H). ^{13}C NMR (125 MHz, $CDCl_3$) δ 13.71, 21.98, 28.48, 30.59, 46.83, 118.72, 129.02, 136.91. IR (ν, cm^{-1}) ν = 3380, 3107.77, 2956–2860, 1654.57, 1507.01; λmax 211.1 nm. GC-EI-MS calculated molecular ion peak for $C_6H_{10}N_2$ 138.21 g/mol, found *m/z* 138 (Figure S4).

*2.3.5. 1-Hexyl-1H-imidazole. (**NHI**).* Yellowish oil. Yield: 62.30%. ^{1}H NMR (500 MHz, $CDCl_3$) δ 0.78 (m, 3H), 1.17 (dd, J = 8.8, 4.1 Hz, 6H), 1.65 (quint, J = 7.2 Hz, 2H), 3.80 (t, J = 7.1 Hz, 2H), 6.80 (s, 1H), 6.92 (s, 1H), 7.35 (s, 1H). ^{13}C NMR (125 MHz, $CDCl_3$) δ 13.87, 22.34, 26.05, 29.39, 30.87, 46.91, 118.80, 129.40, 136.50. IR (ν, cm^{-1}) ν = 3379, 3109, 2955–2858, 1699.5, 1507.81; λmax 212.2 nm. GC-EI-MS calculated molecular ion peak for $C_8H_{14}N_2$ 152.24 g/mol, found *m/z* 152 (Figure S5).

*2.3.6. 1-Otyl-1H-imidazole (**NOI**).* Yellowish oil. Yield: 50.36%. ^{1}H NMR (500 MHz, $CDCl_3$) δ 0.83–0.75 (m, 3H), 1.20 (d, J = 7.9 Hz, 10H), 1.68 (quint, J = 7.2 Hz, 2H), 3.84 (t, J = 7.2 Hz, 2H), 6.82 (s, 1H), 6.95 (s, 1H), 7.38 (s, 1H). ^{13}C NMR (125 MHz, $CDCl_3$) δ 14.01, 22.51, 26.45, 29.28, 31.65, 47.00, 54.40, 69.40, 118.90, 129.00, 136.91. IR (ν, cm^{-1}) ν = 3223, 3112.04, 2956–2855.93, 1701.24, 1508.61; λmax 213.0 nm. GC-EI-MS calculated molecular ion peak for $C_8H_{14}N_2$ 180.29 g/mol, found *m/z* 180 (Figure S7).

*2.3.7. 1-Dexyl-1H-imidazole (**NDI**).* Yellow oil. Yield: 60.50%. ^{1}H NMR (500 MHz, $CDCl_3$) δ 0.80 (t, J = 7.0 Hz, 3H), 1.13–1.24 (m, 14H), 1.69 (quint, J = 7.1,2H), 3.85 (t, J = 7.1 Hz, 2H), 6.84 (s, 1H), 6.97 (s, 1H), 7.40 (s, 1H). ^{13}C NMR (125 MHz, $CDCl_3$) δ 14.02, 22.58, 26.45, 29.28, 30.98, 31.72, 31.77, 47.04, 54.10, 69.30, 118.78, 129.02, 136.91. IR (ν, cm^{-1}) ν=(Data) λmax 211.0 nm. GC-EI-MS calculated molecular ion peak for $C_8H_{14}N_2$ 208.34 g/mol, found *m/z* 208 (Figure S7).

The structures of the alkylimidazoles are shown in Figure 1.

2.4. Antimicrobial assays

2.4.1. Minimum inhibitory concentration

The broth dilution protocol was used in determining the minimum inhibitory concentration (MIC) of the alkyl imidazoles and gentamicin (standard drug). To a sterile nutrient broth, a swab of microorganism in a stabbed agar was added. This was then incubated at 37 °C overnight.

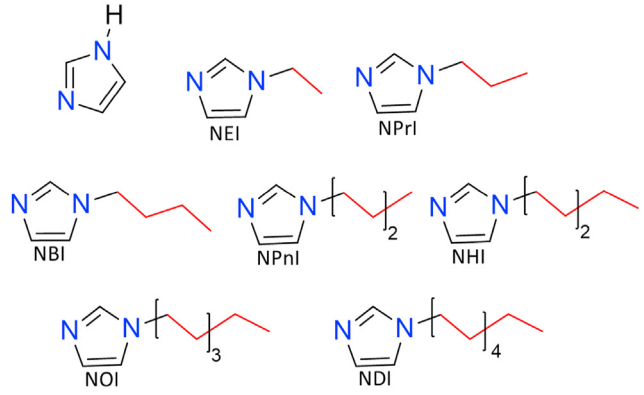

Figure 1. Structures of alkyl imidazoles from Scheme 1; NEI: N-ethylimidazole; NprI: N-propylimidazole; NBI: N-butylimidazole; NpnI: N-pentylimidazole; NHI: N-hexylimidazole; NOI: N-octylimidazole; NDI: N-decylimidazole.

Streaking of the microbial suspension on a sterile nutrient agar was then carried out, followed by incubation at 37 °C overnight. Each overnight microbial culture in sterile saline was adjusted to density commensurate with 0.5 McFarland standard, and this was then added to a double-strength nutrient broth to reach an inoculum size of about 2.0 × 10^5 CFU/mL. Stock solutions of each test compound were prepared in 10% dimethyl sulfoxide (DMSO). All solutions were carefully mixed up until completely dissolved before being used. One hundred microliters of 2-fold serial dilutions of imidazole derivatives or standard (gentamicin) were prepared in a 96-well polypropylene microtiter plate (Thermo Scientific, UK). DMSO (10%) was used as a negative control. One hundred microliters of inoculum were also added to each well to make a total volume of 200 μL, and then allowed to stand at 37 °C for 24 h. MTT (3-(4,5-dimethylthiazol-2-yl)-2,5- diphenyltetrazolium bromide; 20 μL, 1.25 mg/mL) was pipetted into each well and then allowed to stand for 30 min. The MIC was defined as the least concentration of alkyl imidazole that impeded the growth of test organisms, and this was shown by the loss of the purple MTT pigmentation after incubation [24]. Sub-MICs were defined as drug concentrations at which the bacteria growth remained unaffected after 24 h of incubation. All tests were performed in triplicate.

2.4.2. Biofilm inhibition assay

Minimum biofilm inhibitory concentrations of all derivatives were estimated using the anti-biofilm formation assay [25]. An overnight culture of *P. aeruginosa* was made to 0.5 McFarland standard using sterile saline and later, added to a double-strength nutrient broth to reach an inoculum size of ~2.0 × 10^5 CFU/mL. One hundred microliters of the inoculum was added to each well to make a total volume of 200 μL, and then allowed to stand at 37 °C for 24 h. Microtiter plates that contained bacteria without any drug or with sub-MIC doses of compounds or standard drug (gentamicin) were the incubated for 24 h at 37 °C with no agitation. Sub-MIC doses were used to ensure that bacteria could still grow in the presence of test compound and produce biofilms. After 24 h of incubation, the media in each well was removed, and then each well was rinsed with phosphate buffered saline (PBS). Crystal violet (0.1%, v/v) was added to each well and allowed to stand for 3 min. Each stained well was further rinsed with PBS, and then allowed to dry overnight. The attached biofilm on the walls of the wells were re-suspended in 30% (v/v) of glacial acetic acid and transferred into a new sterile plate for absorbance to be measured at 595 nm (BioTeK® Synergy H1 Multi Mode Microplate Reader, Germany). Gentamicin was used as a standard drug. Percentage biofilm inhibition was estimated from the normalized OD values using Eq. (1):

$$\%\ Inhibition = \left(\frac{Control - treated}{Control}\right) \times 100 \quad (1)$$

2.4.3. Pyoverdine quantification

The PA01 strain of *P. aeruginosa* was used for quantifying pyoverdine secretion. *P. aeruginosa* was incubated without any drug (growth control) and also in media supplemented with sub-MIC doses of gentamicin and compounds at 37 °C for 48 h. The cells in each culture media was harvested by centrifuging for 40 min at 4000 rpm. For pyoverdine quantification, 100 μL of the cell-free supernatant was pipetted into a microtiter plate. Fluorescence measurements were carried out at 405 nm for excitation and 465 nm for emission on a BioTeK® Synergy H1 Multimode Microplate Reader (Germany) [15, 25, 26]. Percentage inhibition was computed relative to the control by applying the expression in [1].

2.4.4. Pyocyanin quantification

Pyocyanin quantification was carried out using the *P. aeruginosa* PA01 strain. An inoculum of *P. aeruginosa* was incubated and centrifuged as described in the pyoverdine inhibition quantification assay. Cell-free supernatants were obtained following centrifugation of media

cultures for 45 min at 4000 rpm. To 8 mL of the supernatant solution was added 4 mL of chloroform. The mixture was vortexed 10x for 2 s each. This yielded a green-blue chloroform phase which sunk to the bottom of the tube. Thereafter, the samples were centrifuged at 4000 rpm for 2 min. The supernatant on top of the green-blue chloroform layer was then decanted. Dilute HCl (3 mL, 0.2 M) was then added to each test tube and vortexed for about 2 s. This was repeated 10 times. The content of each test tube was then subjected to centrifugation at 4000 rpm for 2 min. One hundred microliters of the resulting, pink-layered supernatant was transferred into a microtiter plate and absorbance measured at 520 nm [25, 27]. The concentration of pyocyanin was computed from equation [2]

$$\textit{Pyocyanin concentration}\ (\mu g\ /\ mL) = \textit{absorbance at}\ 520\ nm \times 17.072\ (\textit{molar extinction coefficient of pyocyanin at}\ 520\ nm) \quad (2)$$

Evaluation of percentage inhibition was made relative to the control by using the expression in [1].

2.5. Docking studies

3D structures of the ligands (Figure 1) were modeled and optimized with the Hartree Fock approximation using a 3-21G basis set in Spartan '14 V1.1.4. Ligands were further prepared for docking by adding polar hydrogens, merging non-polar hydrogens, and calculating Gasteiger charges for all atoms. The crystal structure of LasR, co-crystallized with the native substrate N-3-oxo-dodecanoyl-L-homoserine lactone, and a quorum sensing anti-activator protein AQS1 [28] was downloaded from the Protein Data Bank with the code 6V7X and a resolution of 2.90 Å. AutoDockTools-1.5.7rc136 was used to prepare the protein for docking by removing crystallographic water molecules and co-crystallized ligands, adding polar hydrogens and calculating Gasteiger charges for all receptor atoms [29, 30].

Molecular docking was performed with Autodock Vina extended in PyRx and UCSF Chimera. Docking in PyRx was used to explore the preferential binding site of the compounds in the protein while that in UCSF Chimera was used to highlight detailed interactions between the protein and ligands. The docking method was validated by redocking the co-crystallized AHL in the binding site. High binding affinities and favorable interactions with critical amino acid residues in the binding site were used to select the best poses [31].

2.6. Data analysis

All graphs and data analysis were done using Microsoft Excel 2019 and GraphPad Prism version 6.0 for Windows (GraphPad Software, San Diego, CA, USA). One-way ANOVA was used to determine significance where needed.

3. Results and discussion

3.1. Chemistry

All compounds were synthesized using Scheme 1. As expected, the IR spectra of the compounds were similar in general. A stretch between 2958 and 2987 cm^{-1} for the sp^3-CH bond typical for an alkyl chain was observed. Also, an sp^2 –CH stretch at 3108 cm^{-1} and an aromatic stretch at 1501 cm^{-1} were present in all compounds and are representative of stretches in the imidazole ring. The ^{1}H-NMR spectra of the compounds showed a singlet in the region 7.38–6.80 ppm which integrates for the protons on the imidazole ring. Variations at the aliphatic regions of both ^{1}H-NMR and ^{13}C were observed due to changes in the length of the alkyl chains. The acidic proton at 13.2 ppm in the ^{1}H-NMR spectrum of imidazole was lost in the ^{1}H-NMR spectrum for all compounds as a result of the substitution of the acidic proton of imidazole with the alkyl group. ^{13}C-NMR of all compounds showed the appearance of a signal in the region 118–138 ppm indicating the presence of an imidazole ring. Also, the appearance of signals ranging from 10 to 69 ppm indicates the presence of the alkyl chains which vary with each compound. The yields of the compounds were between 50 and 65%, and this is similar to the yields reported by another study for the synthesis of similar compounds [20].

3.2. Bacterial susceptibility test

Minimum inhibitory concentrations (MICs) of the compounds against the selected microbes were evaluated in the broth microdilution assay. All compounds exhibited moderate activity against the microbial strains with MICs in the millimolar ranges. A general increase in activity as carbon chain length of substituent alkyl groups on the imidazole ring increased was also observed. The increase in hydrophobicity of the titled compounds is likely responsible for this trend. Hydrophobic groups facilitate better binding to bacterial cellular membranes and hence, offer better chances of antimicrobial activity. The bacterial cell membrane is made up of lipid bilayers and proteins. As a result, the hydrophobic groups are able to interact with bacterial membrane leading to change in the membrane structure which allows permeability of external components into the cytoplasm [32]. The significance of hydrophobicity in antimicrobial action has been reported in a study that assessed the antimicrobial potential of carvacrol and other compounds against different bacterial strains. It was concluded in the study that higher hydrophobicity enables the compounds to interact with the membrane for a period, which alters the membrane permeability [33]. This could be a similar case for the alkylimidazoles. The observed trend in antimicrobial action in this study aligns with the findings from a study conducted by another study where various alkylimidazole compounds exhibited improved microbial action with increase in alkyl chain length [20]. Among the tested microbial strains, the Gram-positive bacteria were more susceptible to the compounds than the Gram-negative bacteria, as seen in Table 1. The thick but porous peptidoglycan cell wall of Gram-positive bacteria permits antimicrobial agents to permeate such bacterial cells. On the other hand, Gram-negative bacteria possess a thin peptidoglycan layer which is further protected by a second outer membrane. This outer membrane serves as an effective barrier to regulate the entry of antimicrobial agents. Moreso, in an event where the outer membrane is ruptured,

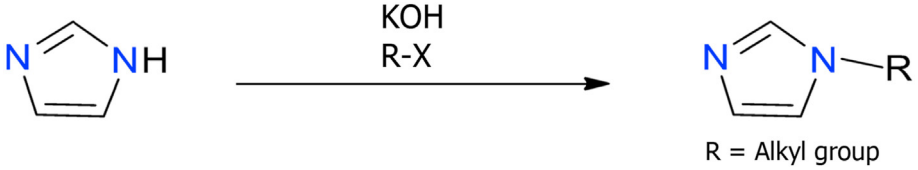

Scheme 1. Synthesis of alkyl imidazoles, R-X = alkyl halide.

Table 1. Minimum inhibitory concentrations of alkyl imidazoles against various microorganisms (mM).

Compounds	*E. coli (-)*	*E. coli* ® *(-)*	*P. aeruginosa PAO1 (-)*	*S. aureus (+)*	*MRSA (+)*	*E. faecalis (+)*
Imidazole	29.41	29.41	29.41	29.41	29.41	29.41
NEI	>104.17	104.17	>104.17	104.17	104.17	104.17
NPrI	18.18	45.45	22.73	18.18	18.18	45.45
NBI	4.03	8.06	16.13	8.06	4.03	16.13
NPnI	1.81	3.62	7.25	3.62	1.81	7.25
NHI	0.82	1.64	3.29	1.64	0.82	3.29
NOI	1.39	1.39	13.02	0.35	5.56	0.69
NDI	1.20	1.20	7.21	0.60	1.20	1.20
Ciprofloxacin	0.00472	0.07545	0.01886	0.00236	0.00236	0.00236
Gentamicin	0.02617	0.05235	0.00654	0.00263	0.05235	0.02617

(+) Gram-positive bacteria, (−) Gram-negative bacteria, (®) Resistant strain.

there is the release of endotoxins that further contribute to the resilience of Gram-negative bacteria and hence makes them more resistant to antimicrobial agents [34]. It has recently been that novel bis-quaternary ammonium compounds were more active against Gram-positive bacteria in comparison to Gram-negative bacteria, similar to observations made here [35]. These outcomes also align with the findings of Kleyi and his team that reveal the marked ability of imidazole-based drugs to show activity against Gram-positive bacteria [36].

The activity of the compounds were also evaluated against some resistant bacterial strains – the multidrug resistant strain of *E. coli* and the methicillin resistant strain of *S. aureus* (MRSA). The MIC for compounds NBI to NDI for these resistant strains were below 10 mM. NHI at 0.82 mM was the best against MRSA whereas NDI was the best against *E. coli*-R at 1.20 mM. Interestingly, NDI inhibited the growth of *E. coli*-R at 1.20 mM which was the same concentration as in the case of MRSA.

Pseudomonas aeruginosa is generally considered as a ubiquitous organism that is common in moist environments with low nutrient availability and ionic strength. This microbe also flourishes in hospital environments and is a predominant causative agent of most nosocomial infections [37]. *P. aeruginosa* is an opportunistic human pathogen that is implicated in cystic fibrosis-related infections and infections in immunocompromised patients [38]. NHI expressed a marked antimicrobial activity against *P. aeruginosa* with an MIC of 3.29 mM. The general difficulty associated with treating *Pseudomonas*-related infections particularly due to the notoriety of the low permeability of the bacterium's outer membranes to antimicrobials. Again, *P. aeruginosa* utilizes several quorum-sensing mediated virulence factors such as pyoverdine and pyocyanin production, and swarming motility as defense mechanisms against antimicrobial agents and stress which regulates biofilm formation.

3.3. Biofilm inhibitory test

Biofilms usually increase the degree of pathogenicity of microorganisms by protecting the cells from external stress or by displaying drug

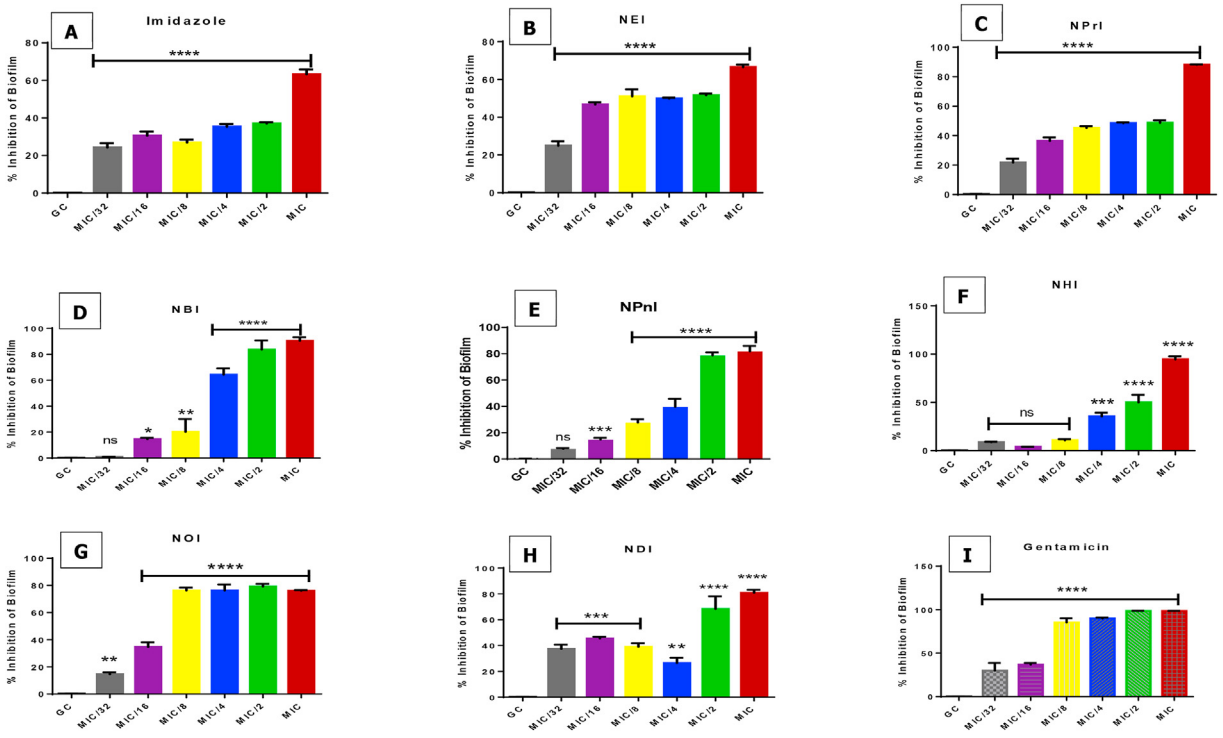

Figure 2. Effect of alkylimidazles on biofilm formation of *P. aeruginosa* at MIC and sub-MIC. Each bar represents mean ± SD of triplicate experiments in a microtiter plate-based assay. Data was subjected to One-way ANOVA followed by Dunnett's *post hoc* test [$p > 0.05$ (ns), $p < 0.05$ (*), $p < 0.01$ (**), $p < 0.001$ (***), $p < 0.0001$ (****), compared to control group], A = Imidazole; B = NEI: N-ethylimidazole; C = NPrI: N-propylimidazole; D = NBI: N-butylimidazole; E = NPnI: N-pentylimidazole; F = NHI: N-hexylimidazole; G = NOI: N-octylimidazole; H = NDI: N-decylimidazole; I = Gentamicin.

tolerance behavior. *P. aeruginosa* is a model pathogen with effective biofilm forming abilities and utilizes this as a means of defense against environmental stress. Biofilms offer bacterial cells up to a thousand-fold increased protection from antibiotic stress [39]. Biofilm inhibition is one of the first lines of defense in controlling the development and survival of surface adherent bacterial populations [26]. The biofilm inhibition properties of the compounds were examined using the crystal violet staining assay. The compounds were evaluated at both MIC and sub-MIC levels. All the compounds exhibited some biofilm inhibition. In general, there was a dose-dependent relationship in the biofilm inhibition pattern for all the compounds (Figure 2). NHI, which was the most active compound against *P. aeruginosa* with an MIC of 3.29 mM (Table 1) inhibited biofilm formation by 94.51% at its MIC. This suggests that NHI has the ability to overcome biofilm formation as part of its action against *P. aeruginosa*. Surprisingly, NOI which had a relatively high MIC against *Pseudomonas* turned out to be the most potent antibiofilm agent with a BIC_{50} value of 0.40 mM. This is an indication of a non-lethal approach to dealing with *P. aeruginosa*. Also, NEI followed suit in this pattern of non-lethal microbial action with a BIC_{50} value of 0.74 mM despite its relatively poor inhibitory activity. Again, similar to NOI, NDI showed better biofilm inhibition activity than NHI although it had a higher MIC against *P. aeruginosa*. A study on N-benzyl derivatives of 4-amino-7--chloro quinolones reported that long chain alkyl derivatives reduced biofilm formation. The most potent agent from our study, NOI, is a long chain alkyl derivative (C-8) and hence agrees with those findings [40]. Alkyl substituted 2-amino imidazole derivatives are examples of imidazole-based compounds that present improved anti-biofilm activity with increase in alkyl chain in *P. aeruginosa* [41], and the data from this work shows that long chain alkyl imidazole exhibits similar traits. Biofilm activities observed for NOI, NDI, and NEI suggest that these compounds are selective in their action i.e., they are capable of inhibiting biofilm formation without affecting the general growth of the organism.

3.4. Inhibition of virulence factors (Pyoverdine and Pyocyanin)

Biofilm formation is a two-stage process that is mostly influenced by surface adhesins and QS [12]. Bacteria have been shown to employ a cascade of signaling events such as QS to modify specific behaviors such as biofilm formation and other virulence potentials [26]. In order to investigate the route by which the alkylimidazoles elicited their antibacterial effect against *Pseudomonas aeruginosa*, we evaluated the effect of the alkylimidazoles on QS-mediated virulence factors, specifically pyoverdine and pyocyanin expression. Treatment with MIC and sub-MIC of test compounds showed a significant difference in percentage inhibition of pyoverdine. Inhibition of pyoverdine expression showed a similar trend as observed in biofilm inhibition; the longer alkyl chains exhibited better pyoverdine inhibitory effect compared to the shorter alkyl chains as observed in the susceptibility tests. At MIC, all the compounds repressed pyoverdine by at least 50% with most of the compounds having greater than 75% inhibitory effect on pyoverdine expression. NHI, the most active compound against *Pseudomonas aeruginosa* from Table 1, inhibited pyoverdine in a dose-dependent manner. NOI as seen in Figure 3, inhibited pyoverdine by at least 60% at all sub-MIC levels. Likewise, NDI inhibited pyoverdine expression by at least 60% at sub-MIC levels. NOI exhibited the overall best inhibitory effect on pyoverdine expression, similar to as observed in biofilm inhibition with percentage inhibition of 88%.

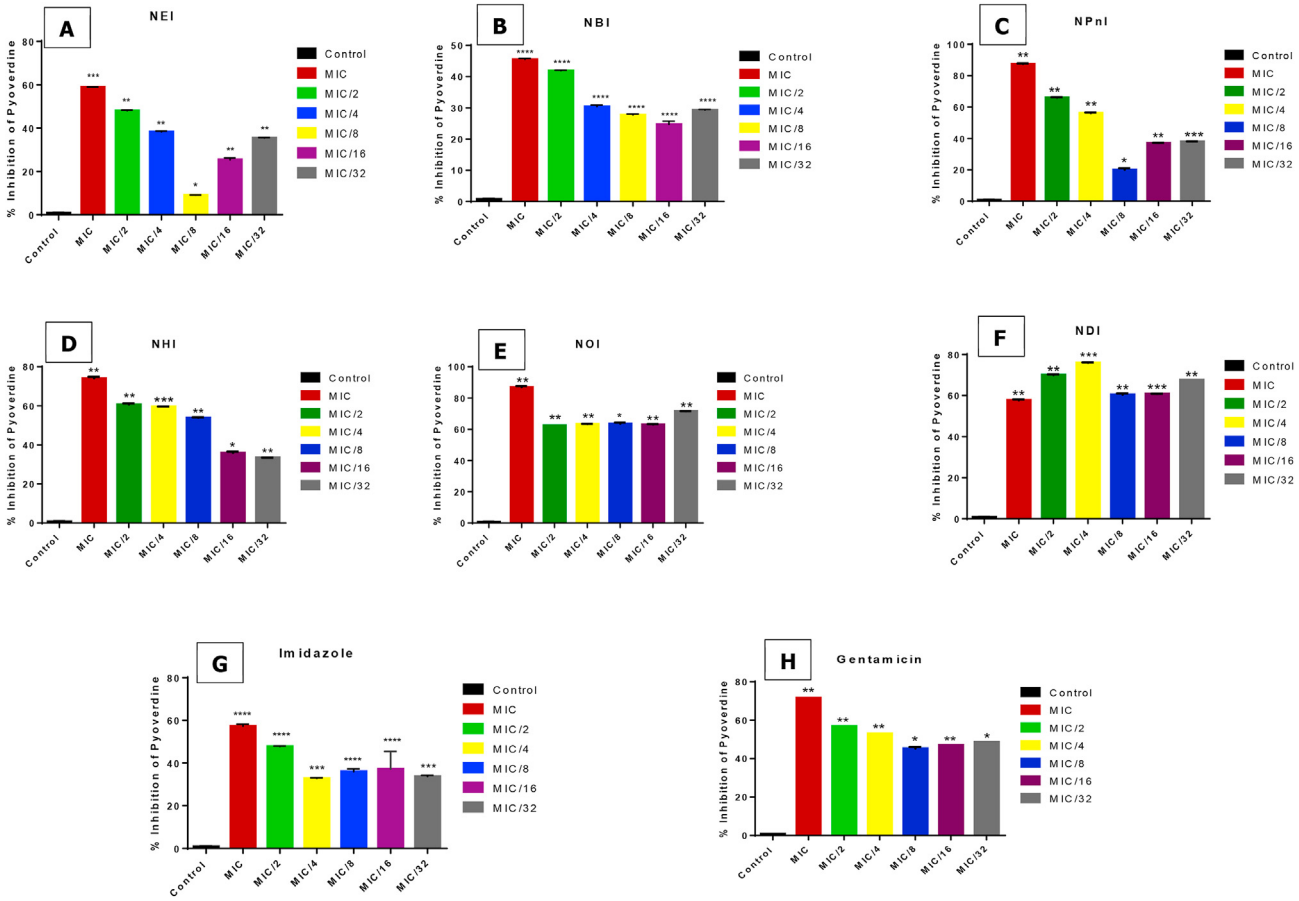

Figure 3. Pyoverdine inhibitory activity of compounds at MIC and sub-MIC doses. Data was subjected to One-way ANOVA followed by Dunnett's *post hoc* test [$p > 0.05$ (ns), $p < 0.05$ (*), $p < 0.01$ (**), $p < 0.001$ (***), $p < 0.0001$ (****), compared to control group], A = NEI: N-ethylimidazole; B = NBI: N-butylimidazole; C = NPnI: N-pentylimidazole; D = NHI: N-hexylimidazole; E = NOI: N-octylimidazole; F = NDI: N-decylimidazole; G = imidazole; H = Gentamicin.

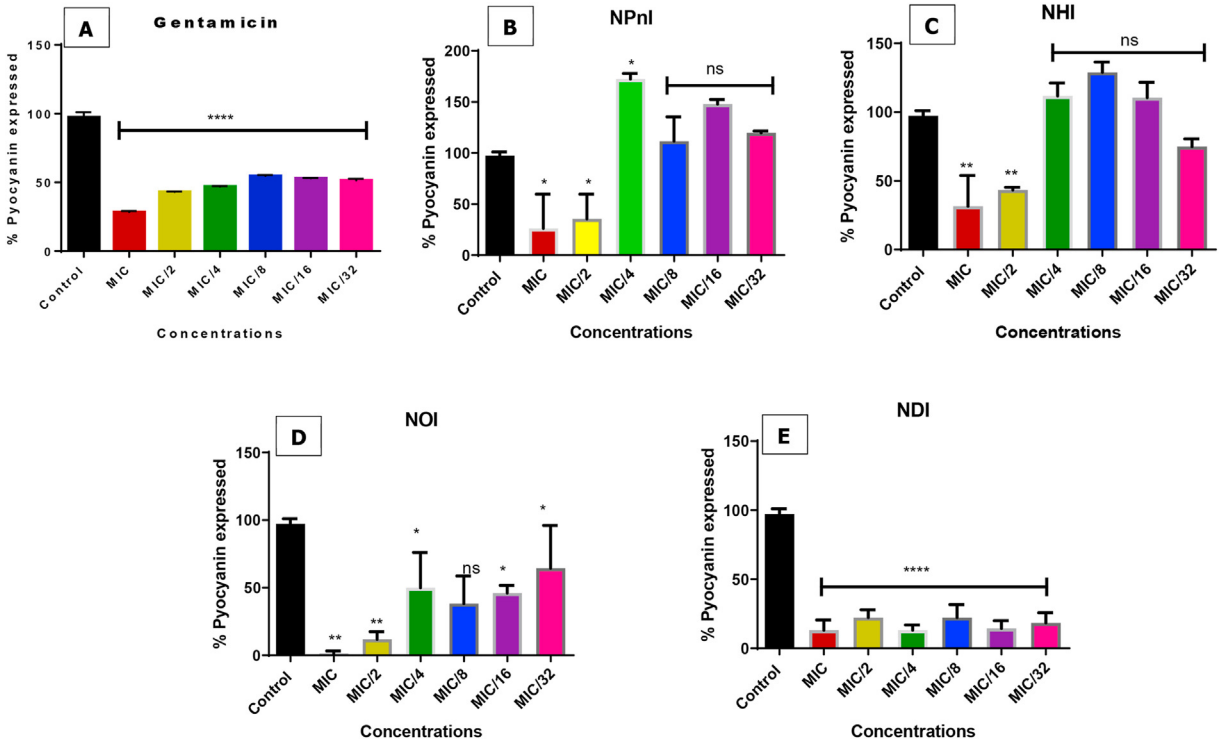

Figure 4. Effect of compounds on pyocyanin inhibition in *P. aeruginosa.* Each bar represent mean ± SD of pyocyanin levels in 3 independent experiments. One-way ANOVA followed by Dunnett's *post hoc* test was carried out. [$p > 0.05$ (ns), $p < 0.05$ (*), $p < 0.01$ (**), $p < 0.001$ (***), $p < 0.0001$ (****), compared to control group], A = Gentamicin; B = NPnI: N-pentylimidazole; C = NHI: N-hexylimidazole; D = NOI: N-octylimidazole; E = NDI: N-decylimidazole.

The inhibition of pyocyanin was evaluated using a UV-visible quantification test. All compounds used in pyocyanin evaluation had greater than 70% effect on pyocyanin expression (Figure 4). Again, longer alkyl chains showed the best inhibitory effect. NOI showed the greatest activity with percentage inhibition of 97.37% at 13.02 mM (MIC). NDI at MIC and sub-MIC doses prevented pyocyanin expression with an average of 81.58%. This observed trend was also observed in the pyoverdine inhibitory assessment where NOI and NDI reduced the expression the most by at least 60%. These findings agree with a study that proposed that longer alkyl chains attached to antimicrobial agents provide better anti-virulence effect against *P. aeruginosa* [40]. The impressive anti-virulence properties exhibited by NOI and NDI may have led to greater biofilm inhibition since cell-to-cell communication contributes to biofilm formation process [12]. Hence, these compounds could act as viable leads for an anti-virulence approach to eradicating multidrug resistance as portrayed by *P. aeruginosa.*

3.5. Molecular docking studies

The QS machinery in *P. aeruginosa* works in a hierarchical fashion, with the las system at the top. Activation of the las system by its autoinducer - acyl homoserine lactone (AHL), the LasR protein multimerizes

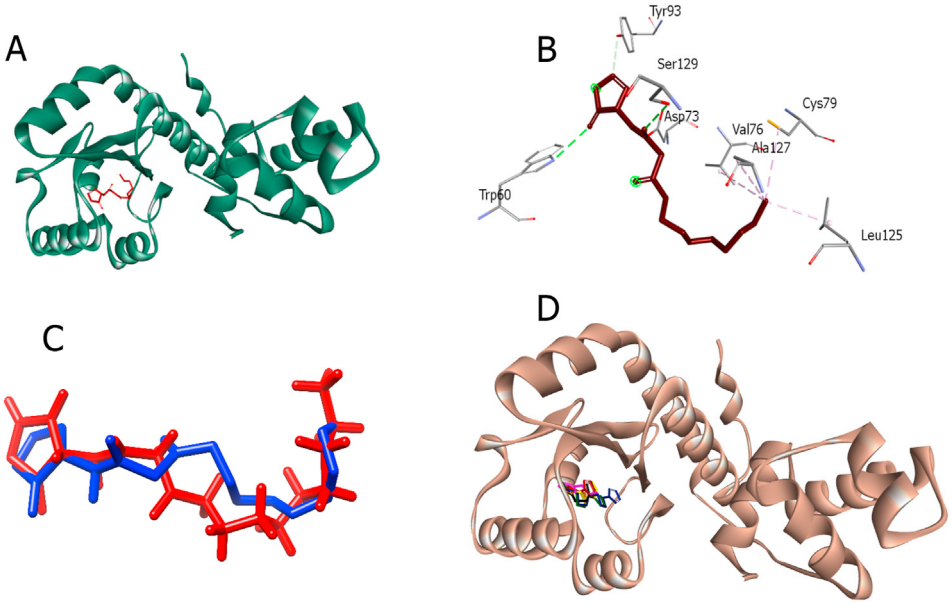

Figure 5. (A) Modified crystal structure of the LasR protein retrieved from the PDB (6v7x) showing AHL in red. (B) 3D illustration of AHL interacting with active site amino acid residues of the LasR protein as retrieved from the PDB. (C) Image of validation – Superimposed representation of redocked AHL (red) and co-crystallised AHL (Blue), RMSD = 1.158 ÅÅ. (D) Image of protein showing all 7 compounds bound at the active site – NEI (Red), NPrI (Brown), NBI (Black), NPnI (Yellow), NHI (Green), NOI (Pink), NDI (Blue).

Table 2. Binding free energies (ΔG) of the compounds docked against the LasR protein (6v7x) with interacting amino acids and their interaction.

Compounds	Binding Energies (ΔG)/kcalmol^{-1}	Hydrogen bond interaction	Hydrophobic interactions
LasR_AHL_complex		Trp60, Asp73, Val76,	Tyr93, Cys79, Leu125, Ala127, Ser129
Re-docked AHL	-8.76	Trp60, Asp73, Thr75	Val76, Cys79, Leu125, Ser129
NDI	-6.90		Leu36, Ile52, Val76, Trp88, Phe101, Ala127
NOI	-6.30		Leu36, Tyr64, Val76, Trp88, Phe101
NHI	-6.10		Leu36, Tyr64, Asp73, Trp88, Phe101
NPnI	-5.80	Thr75	Leu36, Tyr64, Asp73, Trp88, Phe101
NBI	-5.40	Thr75	Leu36, Tyr64, Asp73, Trp88, Phe101
NPrI	-5.00	Thr75	Asp73, Thr75, Trp88, Ala105, Leu110
NEI	-4.50	Leu110	Tyr56, Trp60, Tyr64, Trp88, Phe104, Ala105

and initiates the transcription of RhlR and other virulence factors as part of its regulon [42]. Thus, inhibiting the LasR protein could result in a series of events that could potentially deactivate quorum-sensing and shut down biofilm formation. Molecular docking studies was conducted to ascertain the interactions between the compounds and the protein target LasR. From the structure of LasR (Figure 5), the autoinducer AHL binds to the ligand binding domain by establishing interactions with pocket residues Trp 60, Asp 73, Val 76, Tyr 93, Cys 79, Leu 125, Ala 127, and Ser 129 (Table 2). The polar head of AHL made hydrogen bonds with Trp60, Asp73, and Ser129, and interacted with Val 76, Cys 79, Leu 125, and Ala 127 via its hydrophobic tail group (Figure 5). The stable and precise binding of the AHL depends on the interactions with these residues as they provide directionality and specificity [43]. Potential inhibitors are required to disrupt these interactions, which will change the interior chemistry of the protein and thereby lead to protein aggregation [43]. Blind docking was initially performed using PyRx to search the whole conformational space of the protein and determine the binding site preference of the ligands to it. Results from the blind docking of the molecules against the whole LasR protein revealed that all the molecules were bound in the ligand-binding domain of the protein (Figure 5). This can be attributed to the chemical architecture of the molecules as they share some similarities with the autoinducer of the protein.

From precision docking, NEI, the shortest alkyl chain compound, had a binding affinity of −4.5 kcal/mol (Table 2) with its tail group interacting with Trp 60 via pi-alkyl interaction. A binding affinity of −5.0 kcal/mol was observed for NPrI with its imidazole group interacting with Asp 73 via pi-anion interaction. For NBI, the imidazole head group established pi-anion interaction with Asp 73 while possessing a binding affinity of −5.4 kcal/mol. NPnI and NHI had binding affinities of −5.8 kcal/mol and −6.1 kcal/mol respectively, with a common pi-anion interaction with Asp73 via their imidazole head group. NOI interacted with LasR with a binding affinity of −6.3 kcal/mol and a pi-alkyl interaction with Val 76. For the longest alkyl chain, NDI, a binding affinity of −6.9 kcal/mol was recorded while interacting hydrophobically with Val 76 and Ala 127. From the binding affinities reported, an increase in alkyl chain correlated with an increase in binding affinity, as reported by [44]. This trend was consistent with the experimental data above. A study conducted by [43], shows that two specific ligand-LasR interactions, Trp 60 and Asp 73 via hydrogen bonds, influence a compound as either an agonist or an antagonist. Similar to the autoinducer, hydrogen bond interaction of a ligand with Trp 60 enhances molecular recognition which leads to activation of LasR. This helps to characterize a ligand as an agonist. Compounds that bind at the ligand binding site but form no hydrogen bond interaction with Trp 60 and Asp 73 residues could therefore serve as antagonists of LasR. The alkyl imidazole compounds studied had no hydrogen bond contacts with Trp 60 and Asp 73 (Figures 6 and 7), which suggests that the compounds could act as inhibitors at the binding site. However, due to their low binding affinities as compared to the native autoinducer AHL, they could be classified as weak inhibitors.

The compounds NHI, NOI, and NDI had relatively higher binding affinities to the LasR protein and made interactions with key amino acid residues *in silico* (Figure 7). From the *in vitro* assays, NOI was the most potent in the inhibition of biofilm (Figure 2) and the expression of the QS-

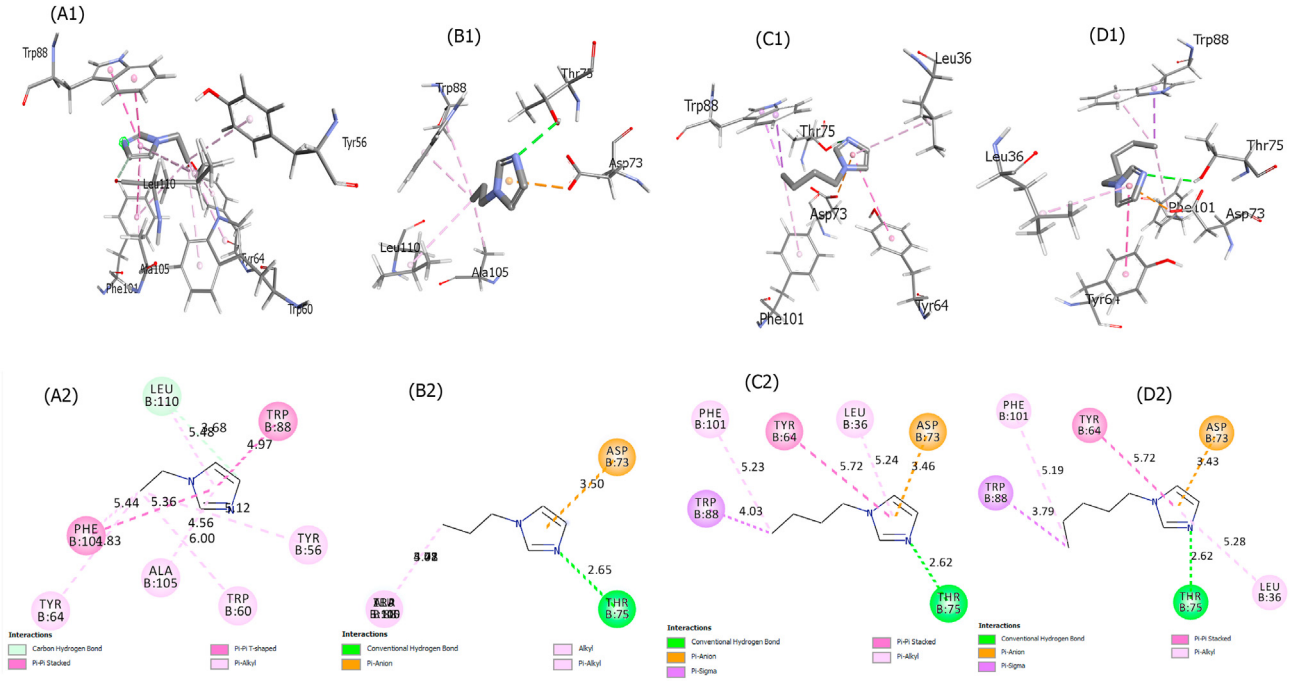

Figure 6. 3D & 2D interactions of alkylimidazole with LasR; (A) ethylimidazole, (B) propylimidazole, (C) butylimidazole, (D) pentylimidazole.

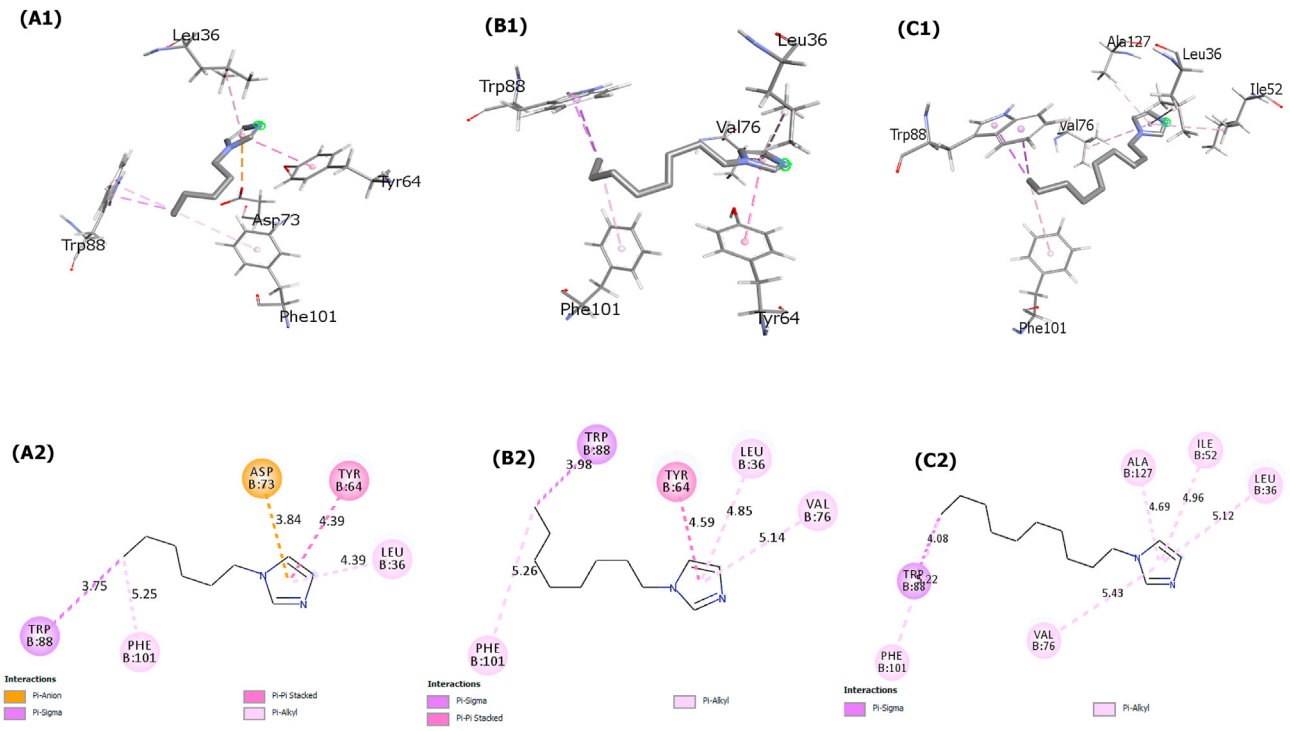

Figure 7. 3D & 2D illustration interactions of alkylimidazole with LasR; (A) hexylimidazole, (B) octylimidazole, (C) decylimidazole.

mediated virulence factors - pyocyanin and pyoverdine. Generally, trends observed in the *in-silico* study corroborated the *in-vitro* findings associated with *Pseudomonas aeruginosa* and its QS-related responses. This contrasts with the findings of [45], who reported that increasing chain length had no correlation with increased biological activity [45]. The difference in findings could be due to different experimental conditions employed for both studies. This highlights the relevance of this study to the development of new therapeutics to combat antimicrobial resistance.

4. Conclusion

In this study, seven compounds were tested against a panel of micro-organisms. The study revealed that alkylimidazole compounds with a chain length of 5 or more could serve as potential inhibitors of the QS-mediated virulence mechanisms used in the biosynthesis of pyocyanin and pyoverdine by *P. aeruginosa*. From the *in vitro assays*, octylimidazole (NOI) and decylimidazole (NDI) emerged as the top candidates as shown in their anti-virulence and biofilm inhibition properties. Notably, the compounds were bacteriostatic against the micro-organisms, which could reduce the likelihood of antimicrobial resistance. *In silico* studies affirmed the assertion made from experiments as the compounds bound favorably at the ligand binding domain and had a good correlation between docking score and QSI activity. Hence, these compounds could be considered as potential warheads in the development of conventional antimicrobials.

Declarations

Author contribution statement

Caleb Nketia Mensah; Gilbert Boadu Ampomah; Jehoshaphat Oppong Mensah; Caleb Impraim Aboagye; Edward Ntim Gasu: Performed the experiments; Analyzed and interpreted the data; Wrote the paper.

Edmund Ekuadzi, PhD; Nathaniel Owusu Boadi, PhD; Lawrence Sheringham Borquaye: Conceived and designed the experiments; Analyzed and interpreted the data; Contributed reagents, materials, analysis tools or data; Wrote the paper.

Funding statement

Dr. Lawrence Sheringham Borquaye was supported by The World Academy of Sciences [19-111 RG/CHE/AF/AC_I].

Data availability statement

Data included in article/supp. material/referenced in article.

Declaration of interest's statement

The authors declare no competing interests.

Additional information

Supplementary content related to this article has been published online at https://doi.org/10.1016/j.heliyon.2022.e12581.

References

[1] WHO. Antimicrobial, Resistance and Primary Health Care, World Health Organization, 2018, pp. 1–12 (Technical Series on Primary Health Care). Report No: WHO/HIS/SDS/2018.57.
[2] M.E. de Kraker, A.J. Stewardson, S. Harbarth, Will 10 million people die a year due to antimicrobial resistance by 2050? PLoS Med. 13 (11) (2016), e1002184.
[3] Centers for Disease Control and Prevention, Antibiotic Resistance Threats in the United States [Internet], Elsevier, 2021–2022 [cited 2022 Apr 10]. Available from: https://www.cdc.gov/antibiotic-use/antibiotic-resistance.html#.
[4] J. O'Neill, Review on antimicrobial resistance, Antimicrob Resist Tackling Crisis Health Wealth Nations 2014 (4) (2014).
[5] R.C. Moellering, Vancomycin-resistant enterococci, Clin. Infect. Dis. 26 (5) (1998) 1196–1199.
[6] B.E. Murray, Vancomycin-resistant enterococci, Am. J. Med. 102 (3) (1997) 284–293.
[7] D.M. Livermore, M. Yuan, Antibiotic resistance and production of extended-spectrum β-Mactamases amongst Klebsiella spp. from intensive care units in Europe, J. Antimicrob. Chemother. 38 (3) (1996) 409–424.
[8] E. Tzelepi, C.H. Magana, E. Platsouka, D. Sofianou, O. Paniara, N.J. Legakis, et al., Extended-spectrum β-lactamase types in Klebsiella pneumoniae and Escherichia coli in two Greek hospitals, Int. J. Antimicrob. Agents 21 (3) (2003) 285–288.

[9] T. Miyoshi-Akiyama, T. Tada, N. Ohmagari, N. Viet Hung, P. Tharavichitkul, B.M. Pokhrel, et al., Emergence and spread of epidemic multidrug-resistant Pseudomonas aeruginosa, Genome Biol. Evol. 9 (12) (2017) 3238–3245.

[10] J.I. Sekiguchi, T. Asagi, T. Miyoshi-Akiyama, A. Kasai, Y. Mizuguchi, M. Araake, et al., Outbreaks of multidrug-resistant Pseudomonas aeruginosa in community hospitals in Japan, J. Clin. Microbiol. 45 (3) (2007) 979–989.

[11] S.J. Projan, New (and not so new) antibacterial targets–from where and when will the novel drugs come? Curr. Opin. Pharmacol. 2 (5) (2002) 513–522.

[12] L. Chen, Y mei Wen, The role of bacterial biofilm in persistent infections and control strategies, Int. J. Oral Sci. 3 (2) (2011) 66–73.

[13] D. López, H. Vlamakis, R. Kolter, Biofilms, Cold Spring Harb Perspect Biol. 2 (7) (2010) a000398.

[14] R.M. Donlan, Biofilm formation: a clinically relevant microbiological process, Clin. Infect. Dis. 33 (8) (2001) 1387–1392.

[15] A. Adonizio, K.F. Kong, K. Mathee, Inhibition of quorum sensing-controlled virulence factor production in Pseudomonas aeruginosa by South Florida plant extracts, Antimicrob. Agents Chemother. 52 (1) (2008) 198–203.

[16] J. Azeredo, N.F. Azevedo, R. Briandet, N. Cerca, T. Coenye, A.R. Costa, et al., Critical review on biofilm methods, Crit. Rev. Microbiol. 43 (3) (2017) 313–351.

[17] T. Rasamiravaka, Q. Labtani, P. Duez, M. El Jaziri, The formation of biofilms by Pseudomonas aeruginosa: a review of the natural and synthetic compounds interfering with control mechanisms, BioMed Res. Int. 2015 (2015).

[18] M.J. Bottomley, E. Muraglia, R. Bazzo, A. Carfì, Molecular insights into quorum sensing in the human pathogen Pseudomonas aeruginosa from the structure of the virulence regulator LasR bound to its autoinducer, J. Biol. Chem. 282 (18) (2007) 13592–13600.

[19] M. Hossain, A.K. Nanda, A review on heterocyclic: synthesis and their application in medicinal chemistry of imidazole moiety, Sci. J. Chem. 6 (5) (2018) 83–94.

[20] S. Khabnadideh, Z. Rezaei, A. Khalafi-Nezhad, R. Bahrinajafi, R. Mohamadi, A.A. Farrokhroz, Synthesis of N-Alkylated derivatives of imidazole as antibacterial agents, Bioorg. Med. Chem. Lett 13 (17) (2003) 2863–2865.

[21] A. Khalafi-Nezhad, M.N. Soltani Rad, H. Mohabatkar, Z. Asrari, B. Hemmateenejad, Design, synthesis, antibacterial and QSAR studies of benzimidazole and imidazole chloroaryloxyalkyl derivatives, Bioorg. Med. Chem. 13 (6) (2005) 1931–1938.

[22] H. Brahmbhatt, M. Molnar, V. Pavić, Pyrazole nucleus fused tri-substituted imidazole derivatives as antioxidant and antibacterial agents, Karbala Int J Mod Sci 4 (2) (2018) 200–206.

[23] S. Demchenko, R. Lesyk, J. Zuegg, A.G. Elliott, Y. Fedchenkova, Z. Suvorova, et al., Synthesis, antibacterial and antifungal activity of new 3-biphenyl-3H-Imidazo [1, 2-a] azepin-1-ium bromides, Eur. J. Med. Chem. 201 (2020), 112477.

[24] E.N. Gasu, H.S. Ahor, L.S. Borquaye, Peptide extract from olivancillaria hiatula exhibits broad-spectrum antibacterial activity, BioMed Res. Int. 2018 (2018), e6010572.

[25] E.N. Gasu, H.S. Ahor, L.S. Borquaye, Peptide mix from Olivancillaria hiatula interferes with cell-to-cell communication in Pseudomonas aeruginosa, BioMed Res. Int. (2019) 2019.

[26] M.C. Das, P. Sandhu, P. Gupta, P. Rudrapaul, U.C. De, P. Tribedi, et al., Attenuation of Pseudomonas aeruginosa biofilm formation by Vitexin: a combinatorial study with azithromycin and gentamicin, Sci. Rep. 6 (1) (2016) 1–13.

[27] N.G. Naga, D.E. El-Badan, H.S. Rateb, K.M. Ghanem, M.I. Shaaban, Quorum sensing inhibiting activity of Cefoperazone and its metallic derivatives on Pseudomonas aeruginosa, Front. Cell. Infect. Microbiol. 11 (2021), 716789.

[28] M. Shah, V.L. Taylor, D. Bona, Y. Tsao, S.Y. Stanley, S.M. Pimentel-Elardo, et al., A phage-encoded anti-activator inhibits quorum sensing in Pseudomonas aeruginosa, Mol. Cell 81 (3) (2021) 571–583.

[29] J.O. Mensah, G.B. Ampomah, E.N. Gasu, A.K. Adomako, E.S. Menkah, L.S. Borquaye, Allosteric Modulation of the Main Protease (MPro) of SARS-CoV-2 by Casticin—insights from molecular dynamics simulations, Chem. Afr. [Internet] (2022) [cited 2022 Jul 25].

[30] L.S. Borquaye, E.N. Gasu, G.B. Ampomah, L.K. Kyei, M.A. Amarh, C.N. Mensah, et al., Alkaloids from Cryptolepis sanguinolenta as potential inhibitors of SARS-CoV-2 viral proteins: an in silico study, BioMed Res. Int. (2020) 2020.

[31] L.K. Kyei, E.N. Gasu, G.B. Ampomah, J.O. Mensah, L.S. Borquaye, An in silico study of the interactions of alkaloids from Cryptolepis sanguinolenta with Plasmodium falciparum Dihydrofolate Reductase and Dihydroorotate Dehydrogenase, J. Chem. (2022) 2022.

[32] A.H. Delcour, Outer membrane permeability and antibiotic resistance, Biochim. Biophys. Acta 1794 (5) (2009) 808–816.

[33] A. Ben Arfa, S. Combes, L. Preziosi-Belloy, N. Gontard, P. Chalier, Antimicrobial activity of carvacrol related to its chemical structure, Lett. Appl. Microbiol. 43 (2) (2006) 149–154.

[34] A.I. Ribeiro, A.M. Dias, A. Zille, Synergistic effects between metal nanoparticles and commercial antimicrobial agents: a Review, ACS Appl. Nano Mater. 5 (3) (2022) 3030–3064.

[35] N. Frolov, E. Detusheva, N. Fursova, I. Ostashevskaya, A. Vereshchagin, Microbiological evaluation of novel bis-quaternary ammonium compounds: clinical strains, biofilms, and resistance study, Pharmaceuticals 15 (5) (2022) 514.

[36] P. Kleyi, R.S. Walmsley, I.Z. Gundhla, T.A. Walmsley, T.I. Jauka, J. Dames, et al., Syntheses, protonation constants and antimicrobial activity of 2-substituted N-alkylimidazole derivatives, S. Afr. J. Chem. 65 (2012) 231–238.

[37] H. Fazeli, R. Akbari, S. Moghim, T. Narimani, M.R. Arabestani, A.R. Ghoddousi, Pseudomonas aeruginosa infections in patients, hospital means, and personnel's specimens, J. Res. Med. Sci. Off. J. Isfahan Univ. Med. Sci. 17 (4) (2012) 332.

[38] S.L. Gellatly, R.E.W. Hancock, Pseudomonas aeruginosa: new insights into pathogenesis and host defenses, Pathog. Dis. 67 (3) (2013) 159–173.

[39] M.R. Wylie, I.H. Windham, F.C. Blum, H. Wu, D.S. Merrell, In vitro antibacterial activity of nimbolide against Helicobacter pylori, J. Ethnopharmacol. 285 (2022), 114828.

[40] I. Aleksic, J. Jeremic, D. Milivojevic, T. Ilic-Tomic, S. Šegan, M. Zlatović, et al., N-benzyl derivatives of long-chained 4-Amino-7-chloro-quionolines as inhibitors of pyocyanin production in Pseudomonas aeruginosa, ACS Chem. Biol. 14 (12) (2019) 2800–2809.

[41] H.P. Steenackers, D.S. Ermolat'ev, B. Savaliya, A. De Weerdt, D. De Coster, A. Shah, et al., Structure- activity relationship of 4 (5)-Aryl-2-amino-1 H-imidazoles, N 1-substituted 2-aminoimidazoles and imidazo [1, 2-a] pyrimidinium salts as inhibitors of biofilm formation by Salmonella Typhimurium and Pseudomonas aeruginosa, J. Med. Chem. 54 (2) (2011) 472–484.

[42] J. Lee, L. Zhang, The hierarchy quorum sensing network in Pseudomonas aeruginosa, Protein Cell 6 (1) (2015) 26–41.

[43] Y. Zou, S.K. Nair, Molecular basis for the recognition of structurally distinct autoinducer mimics by the Pseudomonas aeruginosa LasR quorum-sensing signaling receptor, Chem. Biol. 16 (9) (2009) 961–970.

[44] G.D. Geske, J.C. O'Neill, D.M. Miller, M.E. Mattmann, H.E. Blackwell, Modulation of bacterial quorum sensing with synthetic ligands: systematic evaluation of N-acylated homoserine lactones in multiple species and new insights into their mechanisms of action, J. Am. Chem. Soc. 129 (44) (2007) 13613–13625.

[45] N.N. Biswas, T.T. Yu, Ö. Kimyon, S. Nizalapur, C.R. Gardner, M. Manefield, et al., Synthesis of antimicrobial glucosamides as bacterial quorum sensing mechanism inhibitors, Bioorg. Med. Chem. 25 (3) (2017) 1183–1194.